High flow polypropylene/SEBS composites reinforced with differently treated hemp fibers for injection molded parts

Panaitescu, Denis Mihaela; Vuluga, Zina; Sanporean, Catalina Gabriela; Nicolae, Cristian Andi; Gabor, Augusta Raluca; Trusca, Roxana

Published in:
Composites Part B: Engineering

DOI (link to publication from Publisher):
10.1016/j.compositesb.2019.107062

Publication date:
2019

Document Version
Accepted author manuscript, peer reviewed version

Accepted Manuscript

High flow polypropylene/SEBS composites reinforced with differently treated hemp fibers for injection molded parts

Denis Mihaela Panaitescu, Zina Vuluga, Catalina Gabriela Sanporean, Cristian Andi Nicolae, Raluca Gabor, Roxana Trusca

PII: S1359-8368(19)31247-8

DOI: https://doi.org/10.1016/j.compositesb.2019.107062

Article Number: 107062

Reference: JCOMB 107062

To appear in: *Composites Part B*

Received Date: 28 March 2019

Revised Date: 27 May 2019

Accepted Date: 23 June 2019

Please cite this article as: Panaitescu DM, Vuluga Z, Sanporean CG, Nicolae CA, Gabor R, Trusca R, High flow polypropylene/SEBS composites reinforced with differently treated hemp fibers for injection molded parts, *Composites Part B* (2019), doi: https://doi.org/10.1016/j.compositesb.2019.107062.

High flow polypropylene/SEBS composites reinforced with differently treated hemp fibers for injection molded parts

Denis Mihaela Panaitescu[1]*, Zina Vuluga[1]*, Catalina Gabriela Sanporean[2], Cristian Andi Nicolae[1], Raluca Gabor[1], Roxana Trusca[3]

[1]National Institute of Research and Development in Chemistry and Petrochemistry ICECHIM, 202 Splaiul Independentei, 060021, Bucharest, Romania

[2]Department of Materials and Production, Aalborg University, Fredrik Bajers Vej 5, 9100 Aalborg, Denmark

[3]Science and Engineering of Oxide Materials and Nanomaterials, University Politehnica of Bucharest, 1-7 Gh. Polizu Street, 011061 Bucharest, Romania

*corresponding author: panaitescu@icechim.ro , zvuluga@icechim.ro

Abstract. Polypropylene/hemp fibers (PP/HF) composites for injection molded car parts show several advantages compared to similar composites containing glass fibers (GF), however they have low impact strength, tensile strength and modulus. Here, hemp fibers modified by alkali and alkali-silane treatment were used to reinforce a polypropylene matrix modified with maleic anhydride grafted polypropylene (MAPP) and SEBS. The addition of HF in PP modified with MAPP and SEBS has increased not only the tensile strength and modulus (by 45% and 230%) but also the impact strength. Double tensile strength and triple Young's modulus were obtained in PP composites with alkali-silane treated HF (HFs) in the presence of MAPP and SEBS. Similarly, the HFs led to a significant increase of storage modulus, with about 100% at room temperature and with about 200% at 120 °C. Moreover, the onset degradation temperature increased with 51 ºC for HFs containing composites compared to neat PP. PP/HFs composites modified with MAPP and SEBS showed improved mechanical and thermal properties, being considered as a viable alternative to PP/GF composites for injection molded parts in the automotive industry.

Keywords: A. Polymer-matrix composites (PMCs); B. Mechanical properties; E. Surface treatments

1. Introduction

Natural fiber polymer composites (NFPC) are already used in building, automotive and other industrial applications. Natural fibers (NF) are used especially to reduce the costs and environmental pollution and to impart some properties like better thermal and acoustic insulation, weight reduction or higher flexibility [1-3]. NFPC are considered a suitable choice for some auto interior parts because NF are cheap, available, non-toxic for humans

during manipulation and non-abrasive for tools during processing and they are lighter compared to glass fibers (GF). Flax, hemp, jute, ramie and kenaf are the most studied among NF, especially as substitutes for GF in polymer composites [1,2,4]. These types of NF are characterized by a higher cellulose content and better cellulose microfibrils alignment in the fiber direction which lead to higher Young's modulus and tensile strength besides other structural features [4].

Several limitations of NFPC have been revealed in previous studies [5,6]. NF have lower thermal stability and higher water absorption compared to GF. The low thermal stability of NF compared to inorganic fillers limits the choice of the polymer matrix and, in some cases, the manufacturing process. Besides, the mechanical properties of NFPC are lower than that of GF polymer composites (GFPC) when the same polymer is used as a matrix. Compatibility and polymer/filler interface are challenging for NFPC as for GFPC. Surface modification of NF may overcome some of the NFPC drawbacks [7-9] and several attempts to improve the surface properties of NF by physical or chemical treatments have been reported [7,10-13].

Among NFPC, a special interest was devoted to the study of polypropylene (PP) - hemp fibers (HF) composites [6,9,14-17]. Beckermann and Pickering [14] studied the effect of two alkali treatments of HF (10 wt% NaOH and 5 wt% NaOH/2 wt% Na_2SO_3) on the thermal and mechanical properties of PP-HF composites containing maleic anhydride grafted polypropylene (MAPP) as a coupling agent. The composites were obtained by extrusion - injection molding. Almost no improvement in tensile strength and Young's modulus was observed after the alkali treatment of HF; however an increase of tensile strength was noticed after MAPP addition [14]. Different mechanical response was reported for composite plates containing PP, NaOH treated HF and MAPP, which were prepared using a twin-screw extruder, a low shear plasticator and a compression molding press [6]. Both tensile strength and modulus were higher in the case of the composites with treated HF compared to that containing untreated HF [6]. Etaati et al. [15] have shown that MAPP was efficient as coupling agent in PP-HF composites even in low concentration (2.5 wt%) and maleic anhydride grafted poly(ethylene octane) improved the tensile strength and Young's modulus of PP-HF composites only if used in high concentration. In contrast, no effect of MAPP on the Young's modulus of PP-HF composites was observed by Espinach et al. [16]. The same group reported that the Young's modulus of PP - hemp core fibers composites was not influenced by either alkali treatment or MAPP addition [9,17]. Nevertheless, the tensile strength was improved by the harshening of the alkali

treatment and further addition of MAPP [9]. Simple water washing of HF was also proposed to improve the mechanical properties of PP-HF composites [18].

Organosilanes were extensively studied to improve the properties of NFPC [8,11,19,20]. The treatment of jute fibers with γ-glycidoxypropyl trimethoxy silane (GPS) improved the adhesion between the fibers and PP and increased the tensile properties of composites [19]. In contrast, vinyltrimethoxy silane treatment of flax fibers had no effect on the tensile and flexural strength of PP – flax fibers composites [20]. The literature regarding the influence of silanes in PP-HF composites is scarce [21,22]. HF treated with γ-aminopropyl-triethoxysilane (APS), GPS and γ-methacryloxypropyltrimethoxysilane (MPS), without alkaline pretreatment, had different effect on the mechanical properties of PP-HF composites [21]: MPS treated HF led to higher tensile and nanoidentation moduli compared to untreated HF, smaller improvement was brought by APS treatment and almost no change by GPS one. Moreover, it has been reported that MAPP led to higher interfacial shear strength in PP-HF composites than silane or alkali treatment of HF [8]. On the other hand, a combined alkali and silane (APS) treatment of HF mats was reported as more efficient than a simple alkali treatment [22]. Rachini et al. [11] have shown the advantages of using two organosilanes, one covalently grafted on PP and the other onto HF surface.

The effect of NF concentration and surface treatment on the impact strength (IS) of PP composites is not completely understood [11,23-27]. Incorporation of hemp core fibers (10, 30 and 40 wt%) decreased the IS of the composites, regardless their concentration and no increase of IS was determined by the alkali treatment of the fibers or MAPP addition [24]. Similarly, a strong decrease of IS was reported for recycled PP reinforced with 30 wt% HF and almost no influence of MAPP [25]. Other study has shown that the incorporation of HF (10 – 40 wt%) in PP led to a drastic decrease of IS but the addition of MAPP reduced the difference [26]. Puech et al. [27] measured the propagation of macro-cracks and the force-displacement dynamic response in PP–HF and PPGF composites by using a drop-weight impact machine and a high speed camera. They demonstrated that the PP-HF composite absorbs much more energy, with up to 40% higher than that absorbed by the PPGF composite due to the higher strain at break and different failure mechanism [27].

NFPC are tougher and have a better crushing behavior compared to GFPC, which is a very important property for the automotive industry [5]. However, PP has low impact strength and modulus and the addition of HF may further decrease the impact strength, as discussed above. This prevents the application of PP-HF composites in automotive parts. The addition of SEBS as an impact modifier was proposed in our previous works

to improve the properties of PP composites [28,29]. Nevertheless, the influence of alkali or alkali-silane treatment of HF on the mechanical and thermal properties of PP-SEBS-HF composites was not studied. In this work, PP containing SEBS and MAPP was reinforced with differently treated hemp fibers. The composites were characterized by static and dynamic mechanical tests, thermogravimetric analysis (TGA), differential scanning calorimetry (DSC) and scanning electron microscopy (SEM) to investigate the effect of modifiers and treatments on the morphology and mechanical properties of composites intended for automotive industry.

2. Experimental part

2.1. Materials

High flow polypropylene copolymer BJ380MO (PP) produced by Borealis AG (Austria) with a MFI of 80.0 g/10 min (230 °C/2.16 kg) and a density of 0.906 g/cm^3 was used as matrix. Kraton 1652G (SEBS), a linear poly[styrene-b-(ethylene-co-butylene)-b-styrene] with 29% styrene content, Mn =79,100 and density of 0.91 g/cm^3 was purchased from Kraton Polymers (USA). Maleic anhydride grafted polypropylene (MAPP), Polybond 3200 from Crompton (USA), with a density of 0.91 g/cm^3 and a melting point of 157 °C was used as a coupling agent. Hemp fibers (97% purity) with a length of 15-20 cm were purchased from HempFlax BV Netherlands. APS as Xiameter OFS-6011 from Dow Corning (USA) and sodium hydroxide (NaOH) from Sigma Aldrich (USA) were used as received.

2.2. Treatment of HF

Hemp fibers with a length of 3 - 6 mm (HF) were cut from the original long fibers using a laboratory mill with adjustable die for better feeding and blending in the extruder. Hemp fibers were treated at about 90 °C with 1%NaOH solution in two conditions, for 30 min (1) and for 60 min (2). Alkali treated fibers were washed with water then neutralized with 1 wt% acetic acid solution and washed again with water. The treated fibers (HFh1 and HFh2) were stored at room temperature for several days and then dried in an oven at 80 ºC for 24 h. Part of HFh1 was further treated with APS. A solution of 3% APS in a 90/10 ethanol/water mixture was magnetically stirred at room temperature for 2 h; the pH was adjusted to 5 with acetic acid. HF were added to this solution, kept at room temperature for 2 h, then decanted and dried for 24 h in ambient atmosphere. Silane-treated hemp fibers (HFs) were finally obtained after thermal treatment at 120 °C for one hour.

2.3. Preparation of PP-HF composites

Only alkali treated HF in mild conditions (1), containing small amount of lignin and denoted as HFh, were used for the preparation of composites. This is based on previous studies which have shown the benefic

effect of small amount of lignin in increasing the reinforcing effect of semi-bleached Eucalyptus fibers in polypropylene composites [30] and its compatibilizing effect [31]. Moreover, the complete removal of lignin suppresses the action of π electron interactions between SEBS containing an aromatic moiety and lignin [32], which may lead to better compatibility. Untreated and treated hemp fibers were dried in an oven at 90 ºC for 4 h. PP was mixed with 5 wt% MAPP and 15 wt% SEBS in a rotating mixer for 30 min (room temperature) and the granule mixture was fed in a DSE 20 Brabender Twin Screw Extruder. The fibers were fed in the extruder through a second feeder [28]. Blends and composites with 30 wt% HF were extruded at 160 – 170 ºC at a screw speed of 150 min^{-1} resulting filaments which were cooled and granulated using a pelletizer. Granulated composites were dried in an oven at 80 ºC for 4 h and then injection molded in dumbbell shaped specimens for tensile tests using an injection molding machine (Engel 23/40) at a temperature of 185 °C (Fig. S1). The PP matrix modified with SEBS-MAPP was denoted as PPM. The composites with untreated (HF), alkali (HFh) and alkali-silane treated (HFs) hemp fibers were denoted as PPM 30HF, PPM 30HFh and PPM 30HFs.

2.4. Characterizations

The fractured surfaces of the composites were observed by SEM using a Quanta Inspect F Scanning Electron Microscope (USA) with a field emission gun having a resolution of 1.2 nm at an accelerating voltage of 30 kV. All the samples were frozen in liquid nitrogen and fractured and then sputter-coated with gold for examination. Microscopic investigation of HF was carried out with Olympus BX41 light microscope (Japan) equipped with live view E330 7.5MP Digital SLR Camera and Quick Photo Micro 2.3 software. Images were collected in transmission mode.

Tensile properties of the composites were determined according to ISO 527 using an Instron 3382 Universal Testing Machine. Ten specimens from each composite were tested to determine the tensile properties, five with a speed of 50 mm/min for the tensile strength and five with 2 mm/min for the Young's modulus. The notched Izod impact tests were carried out according to ISO 180 using a Zwick HIT5.5 Pendulum Impact Testers (Zwick Roell AG, Germany) and five specimens for each test. Dynamic mechanical analysis (DMA) was carried out on a TA Instruments DMA Q800 (USA) with a heating rate of 3 °C/min, in dual cantilever mode. Duplicate composite samples were scanned over a temperature range of -85 – 150 °C at a fixed frequency of 1 Hz.

DSC analysis was carried out on a DSC Q2000 from TA Instruments (USA) under helium flow (100 mL/min). Samples (8-10 mg) were heated from room temperature to 200 ºC at a heating rate of 10 ºC/min.

The degree of crystallinity (X_c) of PP was calculated as:

$$X_C = \frac{\Delta H}{\Delta H_0 \; w_{PP}} \cdot 100 \quad (1)$$

where ΔH is the melting enthalpy of the composite, ΔH_0 is the enthalpy of melting of pure crystalline PP (207 J/g - 8,7 kJ/mol, as established by Wunderlich et al. [33]) and w_{PP} is the weight fraction of PP in the composite. The error for the melting enthalpy was ±1 J/g and for temperature ±0.5 ºC.

For thermogravimetric measurements, duplicate samples weighing between 8 and 10 mg were analyzed with a TA-Q5000 V3.13 (TA Instruments, USA) between room temperature and 700 ºC at a heating rate of 10 ºC/min, with nitrogen as purge gas (40 mL/min).

The efficiency of HF treatment was evaluated by attenuated total reflectance (ATR) Fourier Transform Infrared Spectroscopy (FTIR) analysis. Triplicate data were collected for each sample using a TENSOR 37 Spectrometer from Bruker. Measurements were carried out at room temperature from 4000 to 400 cm^{-1}, with 16 scans and a resolution of 4 cm^{-1}.

3. Results and discussion

3.1. Influence of the chemical treatments on HF properties

3.1.1. TGA analysis of HF

TGA data show one major degradation step for all the samples (Fig. 1a). Better thermal stability was observed after the alkali treatments and combined alkali-silane treatment. The degradation of cellulose occurs between 250 °C and 350 °C [34] and has the most important contribution to the main peak observed in the DTG curve of original HF (Fig. 1b).

After the treatments, the main peak was shifted to a temperature higher with about 40 °C compared to untreated HF (Table S1). This shift was caused by the alkali treatment which removed more thermally labile hemicelluloses, other easily hydrolyzed components and some lignin [35]. Indeed, a small shoulder due to the degradation of hemicelluloses was observed at about 243 °C [34] only for untreated HF and not after the treatments. Similarly, an increase of the onset degradation temperature (T_{on}) and temperature at 10% mass loss ($T_{10\%}$) was observed after the alkali treatments and with the intensification of the treatment (Table S1); a similar improvement was noticed after the combined alkali-silane treatment.

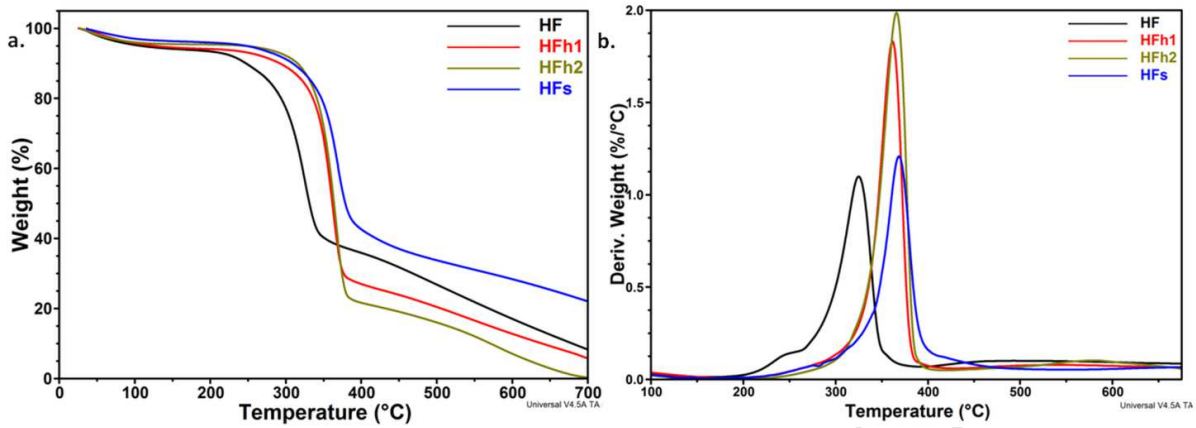

Fig. 1 TGA (a) and DTG (b) curves of differently treated HF

A hump mostly related to the slow degradation of lignin and the formation of char was observed between 400 and 700 °C for HF and only between 500 and 650 °C for HFh2. This was hardly visible for HFh1 and no bump was observed for alkali-silane treated fibers in this temperature range (Fig. 1b), suggesting that the treatments removed a part of lignin. A small shoulder was observed at about 400 °C in the DTG curve of HFs due to polysiloxanes decomposition [36]. It is remarkable the variation of the residue (R_{700}, Table S1), which decreased after the alkali treatments and strongly increased after the alkali-silane treatment. A char residue of 22% was obtained for HFs compared to 8.3 for HF and 5.7 for HFh1. Almost no residue was obtained for HFh2 probably because of the removal of hemicelluloses and great part of lignin after the more intense alkali treatment. Indeed, higher char residue is generated by hemicelluloses and lignin compared to cellulose [34]. A slight increase of the char residue was reported after the silane treatment of neat HF in previous studies [21,28]. Nevertheless, the high residue observed at alkali-silane treated HF was caused by the silane grafted on the surface of HF, which does not decompose up to 700 °C in inert atmosphere, and the presence of polysiloxanes resulted from the condensation of silane [35].

3.1.2. FTIR analysis

The modification of HF by the two alkali treatments (HFh1 and HFh2) determines important structural changes (Fig. 2). The most important changes due to the alkali treatments were observed at about 2900 cm^{-1} (Fig. 2a, detail), this band being assigned to C-H stretching in aliphatic and aromatic structures [34,37,38] and in the region from 1800 to 1500 cm^{-1} (Fig. 2b).

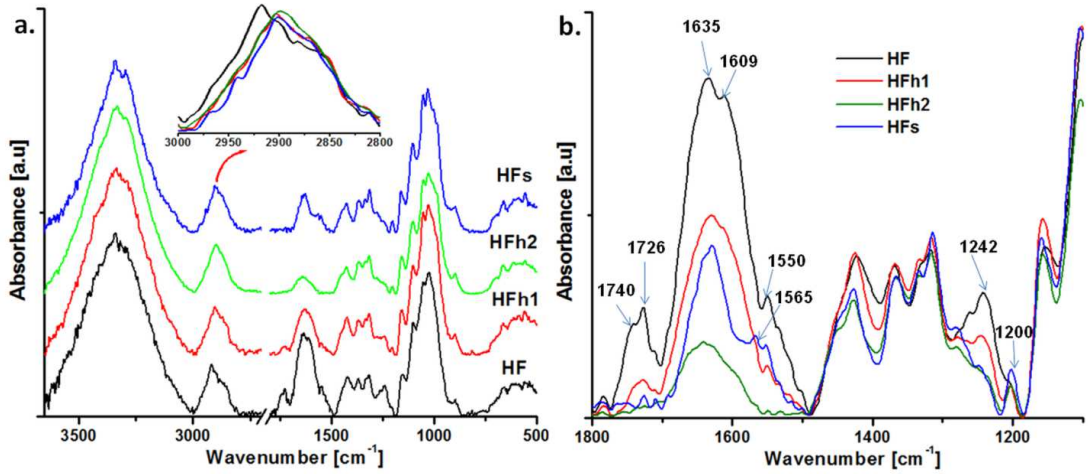

Fig. 2 (a) FTIR spectra (vertically shifted for clarity) of differently treated HF; in the inset - the range from 3000 to 2800 cm^{-1}; (b) FTIR spectra of untreated and treated fibers from 1800 to 1100 cm^{-1}

Untreated HF showed a strong peak at 2918 cm^{-1} and a shoulder at about 2900 cm^{-1}. After the treatments, no peak was observed around 2918 cm^{-1}, regardless the conditions; however a broad peak appeared at 2900 - 2904 cm^{-1} depending on the treatment. The absence of this peak after the alkali treatment may indicate the removal of lignin and enrichment in cellulose. Indeed, lignin shows a strong peak at 2918-2920 cm^{-1} which is ascribed to the C H stretching of methoxyl and methylene groups of lignin [34]. The broad peak at 2900 cm^{-1} is assigned to the C-H asymmetric stretching in the methylene groups of cellulose and hemicelluloses [37]. Harshening of the alkali treatment led to further shift of the peak from 2900 cm^{-1} to lower frequencies probably because of the removal of some hemicelluloses and the corresponding vibrations of the C-H bonds. The shoulders observed at 2879 cm^{-1} and 2860 cm^{-1} in untreated HF (Fig. 2a, detail) and assigned to the C-H stretching in methyl and methylene groups of hemicelluloses and cellulose [38] appeared at lower frequencies after the mild alkali treatment (2872 and 2854 cm^{-1}); this may be also an effect of the partial removal of hemicelluloses.

Untreated HF showed a peak at 1726 cm^{-1} with a shoulder at about 1740 cm^{-1} which is ascribed to the C=O stretching vibration in the carbonyl and unconjugated ketone and carboxyl groups of lignin [34]. The broad signal at about 1740 cm^{-1} may be also attributed to the C=O bond in the acetyl group and in the glucuronic acid side branches of xylan [39]. This peak was strongly attenuated after the mild alkaline treatment (HFh1) and disappeared after the intense alkali treatment (HFh2), showing the removal of most part of lignin and hemicelluloses by the alkali treatment, which is also supported by TGA results. The evolution of the strong peak at

1635 cm^{-1}, which may be related to the C=O stretching vibration in conjugated carbonyl of lignin [40] or to the absorbed water, supports this conclusion: the peak was less intense for HFh2 than for HFh1 (Fig. 2b). In general, both conjugated and unconjugated carbonyl vibrations of lignin decreased with the intensification of alkali treatment conditions. Moreover, the small shoulders at 1609 cm^{-1} and 1550 cm^{-1}, which are assigned to the aromatic skeletal vibrations of phenolic compounds in lignin [41], appeared only in original fibers and more attenuated in HFh1. Another difference was observed in the range from 1280 to 1220 cm^{-1}: a peak appeared at 1242 cm^{-1} only in untreated HF, much attenuated in HFh1 and it was not observed in HFh2. This peak is characteristic to C-O stretching vibrations and it was attributed to lignin [36] and to xyloglucan components of hemicelluloses [42].

The changes observed in the FTIR spectra before and after the alkali treatments highlight the efficiency of the alkali treatments in the removal of hemicelluloses and lignin, the harsher treatment being more effective. However, the HF treated in milder conditions were further modified with silane because the complete removal of lignin is not advantageous [30,31]. A small amount of lignin may improve the reinforcing effect of natural fibers and the interactions between the components, especially in the presence of aromatic polymers [32], such as SEBS. Silane treatment induced further changes: a new peak at 1565 cm^{-1} characteristic to NH_2 bending vibration in aminosilane [43] and a peak at 1200 cm^{-1} corresponding to the "Si-O-cellulose" asymmetric stretching mode [21]. The disappearance of the peaks at 1726/1740 cm^{-1} and at 1242 cm^{-1} shows that most of hemicelluloses and lignin have been removed after the mild alkali treatment combined with silane grafting.

3.2. Influence of the chemical treatments of HF on the properties of PP/HF composites

3.2.1. Mechanical properties of the composites

A slight increase in tensile strength (TS) and double Young's modulus (YM) were observed after the addition of 30 wt% untreated HF in PP (Fig. 3a,b). A 3times decrease of elongation of break (EB) and a decrease of impact strength (IS) with 19% were also observed (Fig. 3e). In the presence of MAPP coupling agent, the influence of HF on the mechanical properties of PP was completely different; the TS increased by 77% and the YM by 146% instead of 20% and 110% in the absence of MAPP. Neat PP and PP/MAPP show similar TS, YM or EB values [28], therefore the strong increase of tensile strength in the composite containing the coupling agent was caused by the improved adhesion at polymer-fiber interface, as reported in previous works [20,26,28]. No

significant change of EB and IS values was observed for the composite containing MAPP (Fig. 3e), they remained lower compared to that of PP.

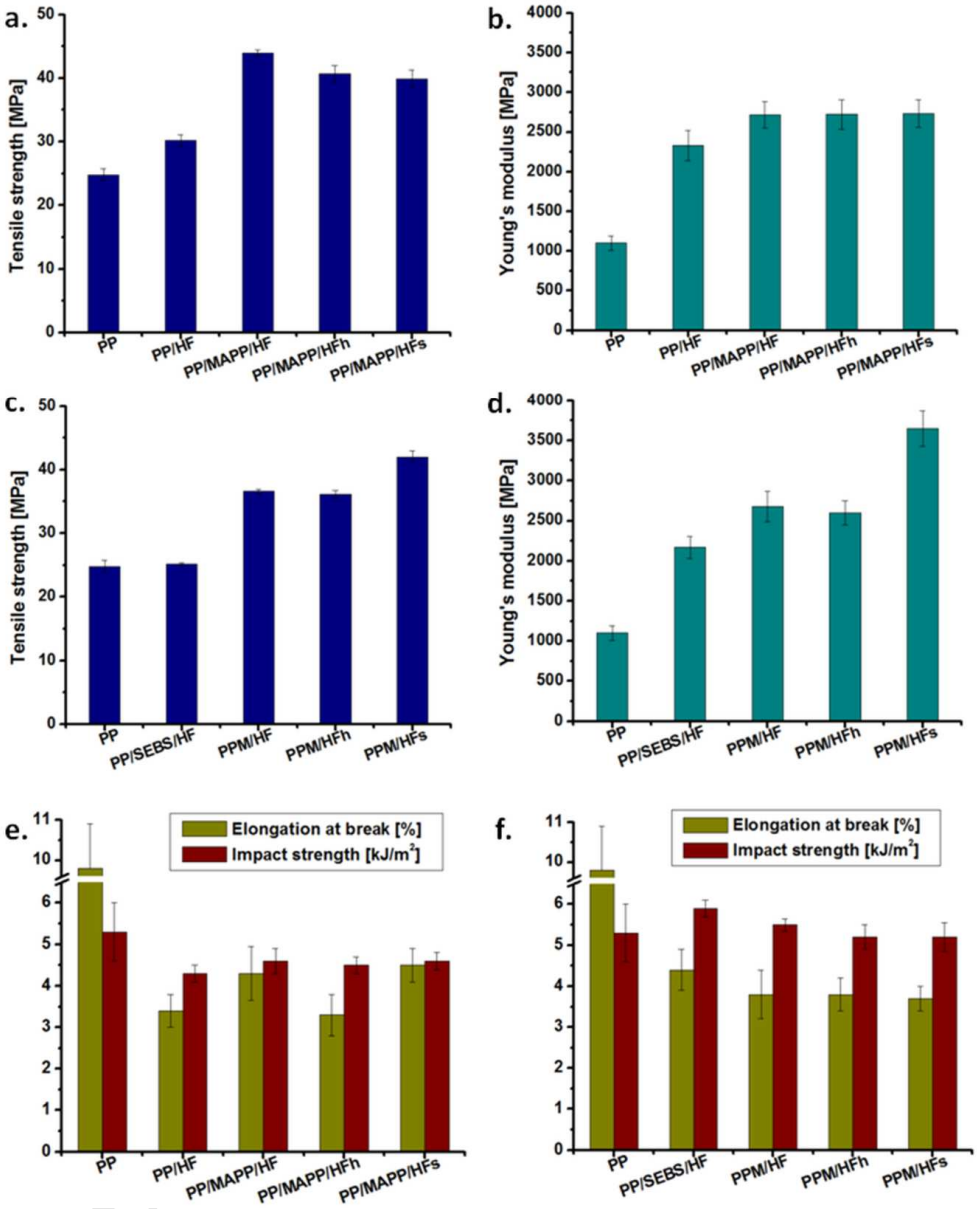

Fig. 3 Tensile strength (a,c), Young's modulus (b,d), elongation at break and impact strength (e,f) of composites with 30 wt% HF, HFh and HFs, with or without SEBS

The treatment of HF by alkali and alkali-silane treatments led to no change in the YM and IS of composites. Nevertheless, a slight decrease in TS was noticed. This unexpected behavior may be caused by several factors: (i) the deterioration of HF after the alkali treatment, (ii) alkali and alkali-silane treatments of HF impede

the action of MAPP coupling agent, (iii) less favorable interface. Regarding the first point, no deterioration of HF was noticed after the alkali treatment by TGA (Fig. 1). Although there is no consensus regarding the effect of alkaline treatment combined with MAPP on the mechanical properties of PP-NF composites [6,9,14-17], it is assumed that NaOH treatment leads to more OH groups on NF surface which are bound to MAPP through hydrogen bonds or ester linkages [9]. Similarly, Panaitescu et al [28] reported better static and dynamic mechanical properties for PP composites containing MAPP and silane treated HF (without any alkaline pre-treatment) compared to PP composites with untreated HF [28]. However, Yeh et al. [44] observed a slight decrease of the tensile strength of PP/MAPP/rice husk composites after the alkali - silane treatment of the fibers. Therefore, different behaviors may result depending on the properties of NF and polymer matrix, the conditions of the treatment and the strength of the fiber-matrix interface. Regarding the interface properties (iii), previous works emphasized the benefic action of lignin [30,31]. Gadioli et al. [30] have shown the advantages of lignin in improving fiber/matrix adhesion in polypropylene/semi-bleached cellulose fibers composites. Moreover, lignin was used as a compatibilizer in hemp-epoxy composites [31]. Therefore, the alkali treatment may increase the proportion of cellulosic OH available to interact with MAPP and the matrix on the one hand and may reduce some possible NF-polymer interactions on the other hand, leading to almost no improvement of the mechanical properties in PP-HF composites.

The addition of SEBS induced several changes in the mechanical behavior of composites (Fig. 3c,d,f). The TS of PP remained, practically, unchanged when SEBS and untreated HF were simultaneously added, because of the opposite effect of the two additives, the stiff HF and the elastomeric SEBS. Interestingly, the YM has doubled in PP/SEBS/HF composite, although the addition of SEBS in PP has a softening effect, decreasing the TS from 24.8 to 19.1 MPa and the YM from 1100 to 760 MPa. The addition of MAPP coupling agent and SEBS in PP/HF composites increased the TS with 47% and the YM with 143%, which is in line with previous results on PP-HF composites [6,9,28]. Nevertheless, the increase of TS was lower than for the composite without SEBS, 47% instead of 77%, due to the elastomeric nature of SEBS [12]. The effect of HFh on the mechanical properties of PPM (PP/SEBS/MAPP) matrix was similar to that observed in the case of PP/MAPP/HFh composite (Fig. 3c,d). However, the effect of HFs was completely different in PPM/HFs compared to the composite without SEBS (PP/MAPP/HFs). The TS was almost double compared to that of PP and the YM increased by 231%. This significant increase in both TS and YM may be related to a strong interface which ensures the transmission of the

effort from the matrix to the fibers [19,25] and a good dispersion of the fibers. The defibrillation of HF following the treatment and the increased contact area may also influence the mechanical behavior of PPM-HFs compared to PPM-HF. Indeed, fibers with a diameter ranging from 50 to 150 µm were observed for original HF and many elementary fibers with a diameter of less than 10 µm and intense defibrillation in the case of HFs (Fig. S2).

The addition of SEBS in PP increased the IS from 5.3 to 9.9 kJ/m^2 but the simultaneous addition of SEBS and HF had a weaker effect and the IS of PP/SEBS/HF composite (6.0 kJ/m^2) was higher but close to that of neat PP. The addition of MAPP, SEBS and surface modified HF had a small effect on the IS which remains close to that of neat PP. It is worth to mention that all the composites containing SEBS showed higher IS compared to the similar composites without SEBS (Fig. 3e,f).

3.2.2. Dynamic mechanical analysis of composites

The effect of HF treatments on the visco-elastic behavior of PP modified with MAPP and SEBS was investigated by DMA. The storage modulus (*E'*) and loss factor (*tan δ*) of the composites as functions of temperature are shown in Fig. 4a,b. PPM exhibited lower storage modulus compared to PP on the whole temperature range due to the increased molecular mobility induced by SEBS addition. The incorporation of HF in PP/MAPP and PPM increased the storage modulus of both matrices (Fig. 4a). However, the increase of *E'* was higher in the case of PPM matrix, regardless the temperature. This shows a better influence of SEBS - MAPP compared to MAPP in PP/HF composites, suggesting a compatibilizing effect of SEBS [12,29]. Indeed, π electron interactions between the residual lignin from HF surface and the aromatic moiety of SEBS [32] on the one hand and entanglements between ethylene-butylene blocks (EB) of SEBS and PP or MAPP [12,14] on the other hand may increase the compatibility (Fig. S3). The incorporation of alkali treated HF in PPM led to lower *E'* values compared to untreated HF, similar to YM decrease. However, the alkali-silane treated HF led to a significant increase of PPM storage modulus, with about 100% at room temperature and with about 200% at 120 °C (Table S2). This is in line with the tensile test results, where YM increased with 230% in PPM/HFs compared to PPM. The concerted action of MAPP and silane coupling agents, multiple entanglements between chains (EB, PP and MAPP) and other possible interactions involving lignin contributed to the formation of a strong interface, which is responsible for the improved mechanical behavior (Fig. S3).

Three relaxations were observed in the *tan δ* vs. temperature plots of PP and PP/MAPP/HF (Fig. 4b); one (12-13 ºC) is related to the glass transition of PP (T_{gPP}), the other at 84 ºC (T_α) is related to the lamellar slip and

rotation in the crystalline phase of PP [45] and the small peak at about -45 ºC is probably coming from some elastomeric segments in the PP copolymer matrix (commercial grade). A low temperature transition was observed at about -47 - -48 °C in PPM and all the composites after the addition of SEBS (Table S3). This transition arises from segmental motions in the ethylene-butylene blocks of SEBS and it was denoted as T_{gSEBS} [46]. No significant change in the glass transition and T_α of PP was observed in composites compared to neat PP, in good agreement with other reports [15,28]. Similarly, almost no variation of the glass transition values for SEBS and PP phases was noticed by DSC (Fig. S4, Table S4).

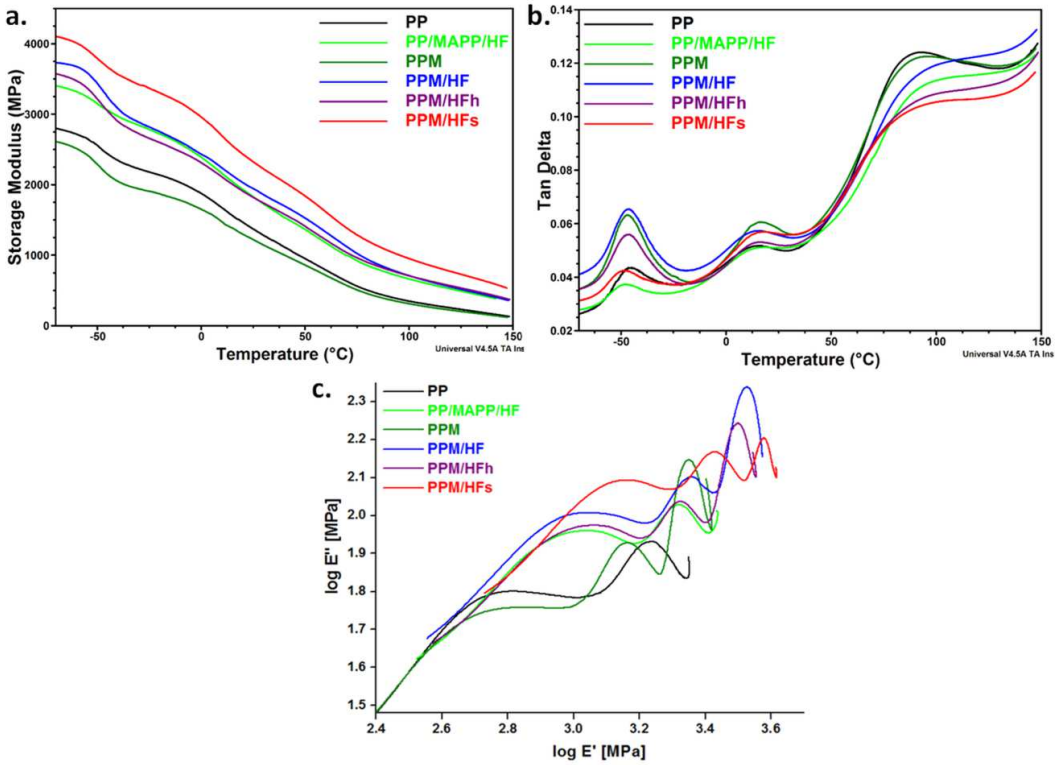

Fig. 4 Storage modulus (a) and tan δ (b) of composites vs. temperature; Cole-Cole plots (c)

The reinforcing effect of HF was estimated by the effectiveness coefficient (C), which is defined by [15]:

$$C = \frac{(E'_G/E'_R)\ composite}{(E'_G/E'_R)\ matrix}$$

where E'_G and E'_R are the storage modulus in the glassy and rubbery region, respectively. The value of the storage modulus at -30 °C was considered for E'_G. The values of C coefficient at two temperatures, 90 and 120 °C, are shown in Table S3. The lowest C value (the highest efficiency) was obtained for PPM/HFs, regardless the temperature. Therefore, alkali-silane treated HF are the most efficient reinforcing agents in PP.

It is remarkable that the height of the *tan δ* peaks corresponding to the glass transition temperatures (T_{gSEBS} and T_{gPP}) in SEBS and PP components of the composites was different depending on the fibers treatment. Higher *tan δ* (SEBS) peak value was noticed for PPM-HF compared to PPM showing poor interface and lower peak heights for PPM-HFh and PPM-HFs, showing better interaction involving SEBS (EB – PP segmental diffusion at interface [47], π electron interactions in lignin – SEBS [32]) (Fig. S3). Therefore, the treatment of the fibers enhanced the interfacial adhesion and reduced the SEBS chains mobility, decreasing the *tan δ* peak [48]. The best interfacial adhesion is reached in the case of PPM-HFs and it is probably determined by the reaction of the amino groups of the silane with the succinic anhydride function of the MAPP at elevated temperature [28] besides other interactions between chains with similar structures. Lower *tan δ* (PP) peak height was observed after the incorporation of HF in PPM, regardless the treatment, showing good fiber – matrix adhesion and low influence of the treatment on PP – HF interface. However, at the Tg of PP (12-15 °C), the frozen PP chains begin to move but the SEBS chains are in a rubbery state, showing high mobility. Therefore, *tan δ* (PP) peak may cumulate several influences related to the dispersion of SEBS and the adhesion at PP - SEBS interface, good dispersion of SEBS and increased adhesion leading to a higher influence of SEBS mobility on the glass transition of PP [49]. The width of the *tan δ* (PP) peak was broader after the addition of untreated and treated HF, which is indicative for an increased heterogeneity. Cole–Cole plots are useful to evaluate the homogeneous/heterogeneous nature of materials [48,50,51]. The logarithmic value of the loss modulus was plotted against the logarithmic value of the storage modulus in Fig. 4c. It is obvious that all the samples are heterogeneous materials. Two arcs plot was observed for neat PP (a copolymer with a two-phase structure) and PP/MAPP/HF, showing the occurrence of two different relaxations [50]. Two arcs in the Cole-Cole plots were also reported for poly(ε-caprolactone)/ poly(lactic acid) blends [50]. Three arcs plots were observed in PPM and all the composites with PPM as matrix. It can be supposed that the new relaxation process is associated with SEBS, which was added in PPM. Multiple arcs in Cole-Cole plots were also reported for differently treated PP/jute yarn commingled composites and explained by the different interfacial effects between the phases [48]. The different position of the plots in the Cole-Cole diagram may be related to the presence of the fibers and to the different interactions between phases [50]. Thus, it is assumed that SEBS and silane treatment increased the compatibility in PP/MAPP/HFs composite, which explains the significant increase of the mechanical properties obtained in this case.

3.2.3. Composite morphology

SEM micrographs (Fig. 5) of the fractured surfaces of polypropylene/hemp fibers composites show different morphologies. The SEM image of PP/HF shows fibers pullout and many big gaps (Fig. 5a), which indicates poor fiber/matrix adhesion.

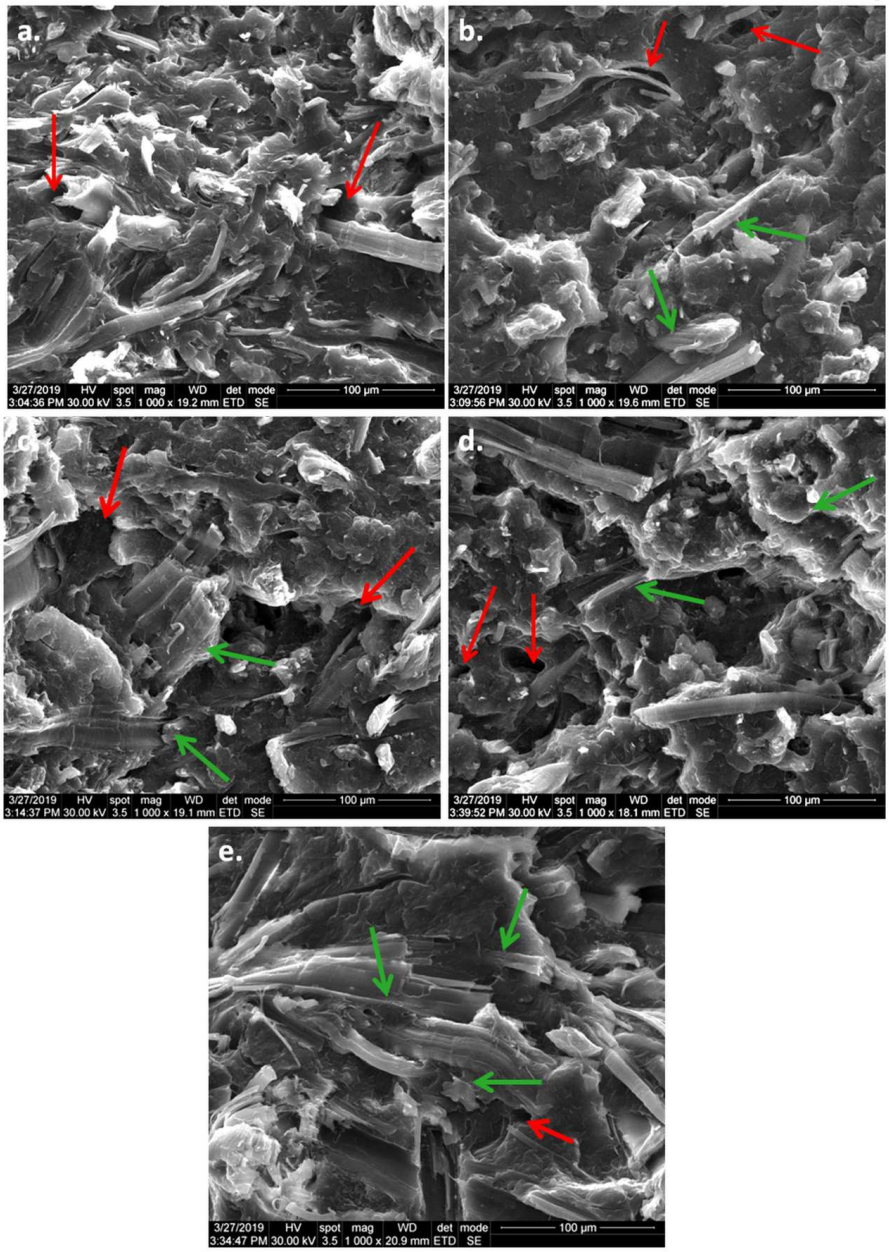

Fig. 5 SEM images of fracture surfaces of PP/HF (a), PP/MAPP/HF (b), PPM/HF (c), PPM/HFh (d) and PPM/HFs(e); red arrows: pullout, debonding or gaps; green arrows: good bonding/adhesion, fibers covered by polymer;

Good fiber/matrix bonding and several gaps were observed in the SEM image of PP/MAPP/HF (Fig. 5b), showing better HF/PP interface adhesion; this is in line with the higher values of tensile strength and modulus obtained for this composite (Fig. 3). Despite the presence of MAPP coupling agent, big gaps and frequent debonding were observed in the SEM images of PPM/HF and PPM/HFh composites (Fig. 5c and d). Therefore, the alkaline treatment of HF is not effective in improving the interface adhesion in PP/HF composites, in line with tensile tests results (Fig. 3). One explanation is the consumption of MAPP at PP/SEBS interface, thus diminishing its contribution at PP/HF interface, as reported in a previous work [28]. Greatly improved fiber/matrix adhesion was observed in Fig. 5e (PPM/HFs), showing the efficiency of the alkali-silane treatment and MAPP addition. This explains the high tensile strength and modulus of this composite compared to neat PP (Fig. 3).

3.2.4. DSC analysis of composites

DSC thermograms of PP composites, first and second melting cycles, are shown in Fig. S5 and the characteristic temperatures and crystallinity in Table 1. The treatment of HF, whatever it was, did not change the aspect of the melting endotherm and the value of the melting temperature in the first as in the second cycle (Fig. S5a). The fusion of PP crystallites occurs between 150 and 170 °C, with a T_{m1} value around 163 °C and a T_{m2} value around 165 °C. The broad endotherms observed in the first melting are probably determined by the thermal history, especially by the rapid cooling in the injection molding machine. The slower cooling (10 ºC/min) during DSC analysis led to sharper endotherms slightly shifted to a higher temperature (T_{m2}, Table 1), indicating better organization of the crystalline phase and thicker crystals.

The incorporation of untreated HF in PP slightly increased the crystallinity (X_C) and the simultaneous addition of HF and SEBS or MAPP led to a higher increase of X_C (10…13%), similar to other observations [12,28]. However, the composites containing both MAPP and SEBS showed much higher crystallinity, with 18…34% higher, depending on the treatment of the fibers. This shows that the nucleating effect of HF was greatly increased by the simultaneous addition of SEBS and MAPP. Other authors consider that, besides the nucleation activity of the filler, the better interfacial stress transfer characteristic to a high compatibility and well-dispersed fillers will also influence the crystallization behavior, increasing the rate of crystallization and crystallinity [52]. Therefore, it may be assumed that SEBS - MAPP addition together with the alkaline-silane treatment ensure a good compatibility in PP-HF composites.

Table 1. DSC results for the composites with different treated HF

Samples	T_c (ºC)	T_{m1} (ºC)	ΔH_{m1} (J/g)	T_{m2} (ºC)	ΔH_{m2} (J/g)	X_c (%)	V (%)
PP	130.6	163.8	84.2	165.2	91.5	44.2	-
PP/HF	129.3	163.1	60.3	164.9	67.7	46.7	+5.7
PP/MAPP/HF	130.1	163.2	62.9	165.0	67.0	49.8	+12.7
PP/MAPP/HFh	130.1	163.2	61.5	164.8	66.7	49.6	+12.2
PP/MAPP/HFs	131.4	163.0	64.8	164.9	67.8	50.4	+14.0
PP/SEBS/HF	129.0	162.9	48.6	164.8	55.1	48.4	+9.5
PPM/HF	129.9	163.0	50.6	164.9	55.4	53.5	+21.0
PPM/HFh	129.5	162.4	50.6	164.3	53.9	52.1	+17.9
PPM/HFs	130.2	162.4	56.0	164.5	61.2	59.1	+33.7

$T_{m1,2}$ – Melting temperature corresponding to the first (1) and second (2) heating cycle;

$\Delta H_{m1,2}$ – Melting enthalpy corresponding to the first (1) and second (2) heating cycle;

X_c – The degree of crystallinity calculated from the second (2) heating cycle;

$V\,(\%) = \frac{X_{c(composit)} - X_{c(PP)}}{X_{c(PP)}} \cdot 100$

The crystallization behavior is similar for all the composites (Fig. S5b) and only small differences in the crystallization temperature, of up to 2.5 °C, were noticed (Table 1); the addition of HF slightly reduced the T_c value, as well the addition of SEBS and the silane treatment increased the T_c value. It may be assumed that the silane treatment led to faster crystallization of PP because of the good compatibility between PP and silane treated fibers, which favors the crystallization of PP melt on HFs surface. The effect of SEBS to hinder the crystallization of PP was previously signaled [29].

3.2.5. Thermal stability

The thermal degradation of neat PP is a single mass loss step with the temperature of the maximum degradation rate (T_d) at 438 °C (Fig. 6a). A small shoulder was observed at a lower temperature in the derivative curves, probably caused by the heterogeneous composition of the PP matrix. A new peak at a lower temperature (327 °C) was observed in the DTG curve of PP/HF composite.

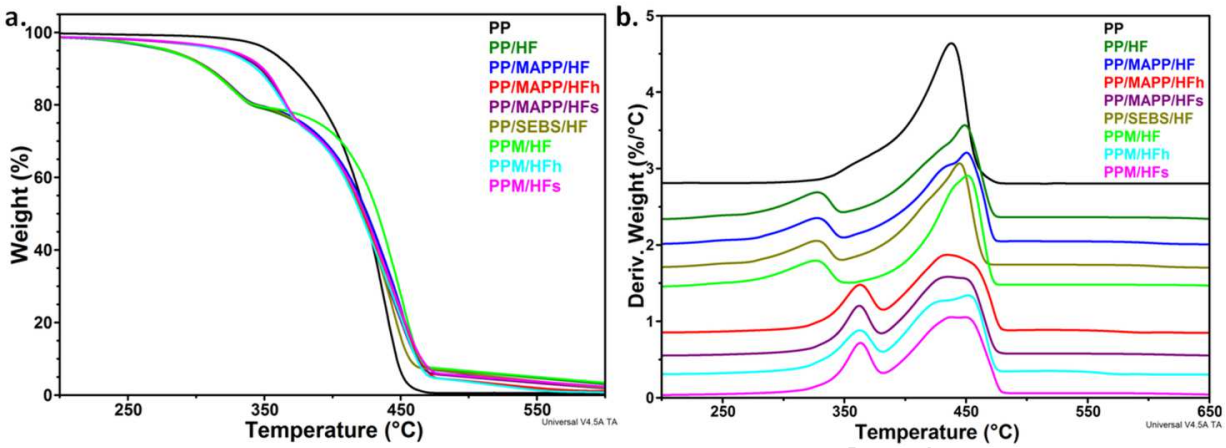

Fig. 6 TGA (a) and DTG (b) curves of PP composites

Although all the composites showed a peak at a lower temperature (T_{df}) because of the degradation of hemp, this peak appeared at a higher temperature for the composites containing treated HF (HFh and HFs) (Table 2). Thus, a peak at 326-327 °C was observed in the case of PP/HF, PP/MAPP/HF, PP/SEBS/HF and PPM/HF (Fig. 6b), mainly due to the degradation of cellulose and a shoulder at about 250 °C corresponding to the degradation of hemicelluloses from the untreated HF. A peak at a higher temperature (362 °C) with no shoulder was observed in the case of PP/MAPP/HFh, PP/MAPP/HFs, PPM/HFh and PPM/HFs. This is caused by the treatment of HF which improved fiber-matrix interactions and removed hemicelluloses with a lower thermal stability [11,12,14].

Table 2. TGA results for PP composites with differently treated HF

Samples	T_{on} (ºC)	T_{df} (ºC)	T_d (ºC)
PP	396.7	-	438.0
PP/HF	291.0	327.5	449.0
PP/MAPP/HF	290.7	327.1	450.6
PP/MAPP/HFh	338.6	362.1	440.7
PP/MAPP/HFs	340.3	361.8	430.2/448.2
PPM	291.5	326.8	444.8
PPM/HF	291.3	325.9	451.4
PPM/HFh	335.3	362.0	427.0/452.6
PPM/HFs	342.1	362.9	438.1/452.9

Another difference between PP and composites is the higher T_d value obtained for composites (448-453 °C) compared to neat PP which was caused by the barrier effect of carbonized HF [28]. The main peak is mostly characteristic to the degradation of PP however, the bifurcation of this peak for the composites containing treated HF suggests some overlapping of PP degradation with that of cellulose due to the good interface.

The results from Table 2 show the efficiency of the HF treatments in increasing the stability of the composites. Thus, the onset degradation temperature is about 340 ºC for the composites with treated HF and only 290 ºC for PP reinforced with untreated HF. PP composites containing HFs showed the highest T_{on} value due to the fibers protection induced by the silane coupling agent [11].

4. Conclusions

Hemp fibers modified by alkali and alkali-silane treatment were used to reinforce a polypropylene matrix modified with MAPP and SEBS. Alkali and alkali-silane treatments removed most of hemicelluloses and lignin from HF surface and increased their thermal stability. The effect of fibers treatments and MAPP coupling agent and the cumulate effect of MAPP, SEBS and surface treatments on the properties of PP were evaluated by static and dynamic mechanical tests and thermal analyses. In the presence of MAPP coupling agent, the TS of PP/HF composite increased by 77% and the YM by 146% instead of 20% and 110% in the absence of MAPP, however lower EB and IS compared to that of PP were noticed. No change in the YM and IS of the composites containing MAPP was caused by alkali and alkali-silane treatments of HF. The addition of HF in PP modified with MAPP and SEBS has increased not only the tensile strength and modulus (by 45% and 230%) but also the impact strength, which is a special feature of PP/MAPP/SEBS/HF composites. The most significant effect on the mechanical properties of PP (double TS, triple YM) was obtained with alkali-silane treated HF in the presence of MAPP and SEBS due to the strong interface and defibrillation of HF. DMA results also confirmed the benefic influence of alkali-silane treatment of HF and SEBS addition. PP composites with treated HF showed better thermal stability, the onset degradation temperature increased from 291 ºC for PP reinforced with untreated HF to 342 ºC for alkali-silane treated HF containing composites. The improved mechanical and thermal properties of PP/MAPP/SEBS/HFs composite make this NFPC a viable alternative to GFPC for injection molded parts in the automotive industry.

Acknowledgement

This work was supported by a grant of the Ministry of Research and Innovation, CNCS-UEFISCDI, ChemErgent, contract no. 23N/2019 within Program NUCLEU and by the European Community's Seventh Framework Programme under grant agreement 314744 (EVOLUTION).

References

1. Sanjay MR, Madhu P, Jawaid M, Senthamaraikannan P, Senthil S, Pradeep S. Characterization and properties of natural fiber polymer composites: A comprehensive review. J Clean Prod 2018; 172:566-581.
2. Faruk O, Bledzki AK, Fink H-P, Sain M. Biocomposites reinforced with natural fibers: 2000-2010. Progr Polym Sci 2012; 37:1552-1596.
3. Al-Oqla FM, Sapuan SM. Natural fiber reinforced polymer composites in industrial applications: feasibility of date palm fibers for sustainable automotive industry. J Clean Prod 2014; 66:347-354.
4. Pickering KL, Aruan Efendy MG, Le TM. A review of recent developments in natural fibre composites and their mechanical performance. Compos Part A 2016; 83:98–112.
5. Monteiro SN, Calado V, Rodriguez RJS, Margem FM. Thermogravimetric behavior of natural fibers reinforced polymer composites-An overview. Mater Sci Eng A 2012; 557:17–28.
6. Sullins T, Pillay S, Komus A, Ning H. Hemp fiber reinforced polypropylene composites: The effects of material treatments. Compos Part B 2017; 114:15-22.
7. Kalia S, Dufresne A, Cherian BM, Kaith BS, Averous L, Njuguna S, Nassiopoulos E. Cellulose-based bio- and nanocomposites: A review. Int J Polym Sci 2011; 8:837875.
8. Park J-M, Quang ST, Hwang B-S, DeVries KL. Interfacial evaluation of modified jute and hemp fibers/polypropylene (PP)-maleic anhydride polypropylene copolymers (PP-MAPP) composites using micromechanical technique and nondestructive acoustic emission. Compos Sci Tech 2006; 66:2686–2699.
9. Del Rey R, Serrat R, Alba J, Perez I, Mutje P, Espinach FX. Effect of sodium hydroxide treatments on the tensile strength and the interphase quality of hemp core fiber-reinforced polypropylene composites. Polymers 2017; 9:377.
10. Ragoubi M, Bienaimé D, Molina S, George B, Merlin A. Impact of corona treated hemp fibres onto mechanical properties of polypropylene composites made thereof. Ind Crops Prod 2010; 31:344–349.
11. Rachini A, Mougin G, Delalande S, Charmeau J-Y, Barrès C, Fleury E. Hemp fibers/polypropylene composites by reactive compounding: Improvement of physical properties promoted by selective coupling chemistry. Polym Degrad Stab 2012; 97:1988-1995.
12. Pracella M, Chionna D, Anguillesi I, Kulinski Z, Piorkowska E. Functionalization, compatibilization and properties of polypropylene composites with hemp fibres. Compos Sci Tech 2006; 66:2218–2230.
13. Borsa J, Laszlo K, Boguslavsky L, Takacs E, Racz I, Toth T, Szabo D, Effect of mild alkali/ultrasound treatment on flax and hemp fibres: the different responses of the two substrates. Cellulose 2016; 23:2117–2128.
14. Beckermann GW, Pickering KL. Engineering and evaluation of hemp fibre reinforced polypropylene composites: Fibre treatment and matrix modification. Compos Part A 2008; 39:979–988.

15. Etaati A, Pather S, Fang Z, Wang H. The study of fibre/matrix bond strength in short hemp polypropylene composites from dynamic mechanical analysis. Compos Part B 2014; 62:19–28.
16. Espinach FX, Julian F, Verdaguer N, Torres L, Pelach MA, Vilaseca F, Mutje P. Analysis of tensile and flexural modulus in hemp strands/polypropylene composites. Compos Part B 2013; 47:339–343.
17. Vilaseca F, Del Rey R, Serrat FR, Alba BJ, Perez I, Mutje P, Espinach FX. Macro and micro-mechanics behavior of stifness in alkaline treated hemp core fibres polypropylene-based composites. Compos Part B 2018; 144:118–125.
18. Han HC, Gong XL. One-step green treatment of hemp fiber used in polypropylene composites. Polym Compos 2016; 37:385–390.
19. Hong CK, Hwang I, Kim N, Park DH, Hwang BS, Nah C. Mechanical properties of silanized jute–polypropylene composites. J Ind Eng Chem 2008; 14:71–76.
20. Arbelaiz A, Fernandez B, Cantero G, Llano-Ponte R, Valea A, Mondragon I. Mechanical properties of flax fibre/polypropylene composites. Influence of fibre/matrix modification and glass fibre hybridization. Compos Part A 2005; 36:1637–1644.
21. Panaitescu DM, Nicolae CA, Vuluga Z, Vitelaru C, Sanporean CG, Zaharia C, Florea D, Vasilievici G. Influence of hemp fibers with modified surface on polypropylene composites. J Ind Eng Chem 2016; 37:137-146.
22. Ma L, He L, Zhang L. Effect of surface treatments on tensile properties of hemp fiber reinforced polypropylene composites. In: Proceedings of AIP Conference 2017. p.1829.
23. Panthapulakkal S, Sain M. Injection-molded short hemp fiber/glass fiber- reinforced polypropylene hybrid composites-mechanical, water absorption and thermal properties. J Appl Polym Sci 2007; 103:2432–2441.
24. Ngaowthong C, Rungsardthong V, Siengchin S. Polypropylene/hemp woody core fiber composites: Morphology, mechanical, thermal properties, and water absorption behaviors. Adv Mech Eng 2016; 8(3):1–10.
25. Kakroodi AR, Leduc S, Rodrigue D. Effect of hybridization and compatibilization on the mechanical properties of recycled polypropylene-hemp composites. J Appl Polym Sci 2012; 124:2494–2500.
26. Yan ZL, Wang H, Lau KT, Pather S, Zhang JC, Lin G, Ding Y. Reinforcement of polypropylene with hemp fibres. Compos Part B 2013; 46:221–226.
27. Puech L, Ramakrishnan KR, Le Moigne N, Corn S, Slangen PR, Le Duc A, Boudhani H, Bergeret A. Investigating the impact behaviour of short hemp fibres reinforced polypropylene biocomposites through high speed imaging and finite element modeling. Compos Part A 2018; 109:428–434.
28. Panaitescu DM, Vuluga Z, Ghiurea M, Iorga M, Nicolae C, Gabor R. Influence of compatibilizing system on morphology, thermal and mechanical properties of high flow polypropylene reinforced with short hemp fibers. Compos Part B 2015; 69:286–295.
29. Panaitescu DM, Vuluga Z, Notingher PV, Nicolae C. The effect of poly[styrene-b-(ethylene-co-butylene)-b-styrene] on dielectric, thermal, and morphological characteristics of polypropylene/silica nanocomposites. Polym Eng Sci 2013; 53(10):2081–92.
30. Gadioli R, Morais JA, Waldman WR, De Paoli MA. The role of lignin in polypropylene composites with semi-bleached cellulose fibers: Mechanical properties and its activity as antioxidant. Polym Degrad Stab 2014; 108:23-34.
31. Wood BM, Coles SR, Maggs S, Meredith J, Kirwan K. Use of lignin as a compatibiliser in hemp/epoxy composites. Compos Sci Tech 2011; 71:1804–1810.

32. Szabó G, Romhányi V, Kun D, Renner K, Pukánszky B. Competitive interactions in aromatic polymer/lignosulfonate blends. ACS Sustainable Chem Eng 2017; 5:410−419.
33. Bu H-S, Cheng SZD, Wunderlich B. Addendum to the thermal properties of polypropylene. Makromol Chem Rapid Commun 1988; 9:75-77.
34. Kabir MM, Wang H, Lau KT, Cardona F. Effects of chemical treatments on hemp fibre structure. Appl Surf Sci 2013; 276:13–23.
35. Norul Izani M-A, Paridah MT, Anwar UMK, MY Mohd Nor, H'ng PS. Effects of fiber treatment on morphology, tensile and thermogravimetric analysis of oil palm empty fruit bunches fibers. Compos Part B 2013; 45:1251-1257.
36. Loof D, Hiller M, Oschkinat H, Koschek K. Quantitative and qualitative analysis of surface modified cellulose utilizing TGA-MS. Materials 2016; 9:415.
37. Nelson ML, O'Connor RT. Relation of certain infrared bands to cellulose crystallinity and crystal lattice type. Part II. A new infrared ratio for estimation of crystallinity in celluloses I and 11. J Appl Polym Sci 1964; 8:1325-1341.
38. Socrates, G. Infrared and Raman characteristic group frequencies. John Wiley & Sons, 2001, p.50–67.
39. Dammström S, Salmén L, Gatenholm P. On the interactions between cellulose and xylan, a biomimetic simulation of the hardwood cell wall. BioResources 2009; 4(1):3-14.
40. Shi J, Li J. Metabolites and chemical group changes in the wood-forming tissue of pinus koraiensis under inclined conditions. BioResources 2012; 7(3):3463-3475.
41. Schwanninger M, Rodrigues JC, Pereira H, Hinterstoisser B. Effects of short-time vibratory ball milling on the shape of FT-IR spectra of wood and cellulose. Vib Spectrosc 2004; 36:23–40.
42. Conzatti L, Brunengo E, Utzeri R, Castellano M, Hodge P, Stagnaro P. Macrocyclic oligomers as compatibilizing agent for hemp fibres/biodegradable polyester eco-composites. Polymers 2018; 146:396-406.
43. Arbelaiz A, Trifol J, Peña-Rodriguez C, Labidi J, Eceiza A. Modification of poly(lactic acid) matrix by chemically modified flax fiber bundles and poly(ethylene glycol) plasticizer. In: Visakh PM, Lüftl S, editors. Polyethylene-based Biocomposites and Bionanocomposites. Scrivener Publishing LLC, 2016. p.429–446.
44. Yeh S-K, Hsieh C-C, H-C Chang, Yen CCC, Chang Y-C. Synergistic effect of coupling agents and fiber treatments on mechanical properties and moisture absorption of polypropylene–rice husk composites and their foam. Compos Part A 2015; 68:313–322.
45. Verma P, Verma M, Gupta A, Chauhan SS, Malik RS, Choudhary V. Multi walled carbon nanotubes induced viscoelastic response of polypropylene copolymer nanocomposites: Effect of filler loading on rheological percolation. Polym Test 2016; 55:1-9.
46. Chen H, Hassan MK, Peddini SK, Mauritz KA. Macromolecular dynamics of sulfonated poly(styrene-b-ethylene-ran-butylene-b-styrene) block copolymers by broadband dielectric spectroscopy. Eur Poly J 2011; 47:1936–1948.
47. Abreu FOMS, Forte MMC, Liberman SA. SBS and SEBS block copolymers as impact modifiers for polypropylene compounds. J Appl Polym Sci 2005; 95: 254.
48. George G, Tomlal Jose E, Akesson D, Skrifvars M, Nagarajan ER, Joseph K. Viscoelastic behaviour of novel commingled biocomposites based on polypropylene/jute yarns. Compos Part A 2012; 43:893–902.
49. Ornaghi HL Jr., Bolner AS, Fiorio R, Zattera AJ, Amico SC. Mechanical and dynamic mechanical analysis of hybrid composites molded by resin transfer molding. J Appl Polym Sci 2010; 118:887–896.

50. Wu D, Zhang Y, Yuan L, Zhang M, Zhou W. Viscoelastic interfacial properties of compatibilized poly(ε-caprolactone)/polylactide blend. J Polym Sci Part B 2010; 48:756–765.
51. Joseph PV, Mathew G, Joseph K, Groeninckx G, Thomas S. Dynamic mechanical properties of short sisal fibre reinforced polypropylene composites. Compos Part A 2003; 34:275-290.
52. Zhang MQ, Rong MZ, Ruan WH. Chapter 3. Nanoparticles/Polymer composites: fabrication and mechanical properties. In: Karger-Kocsis J, Fakirov S, editors. Nano- and Micromechanics of Polymer Blends and Composites. Carl Hanser Verlag GmbH & Co. KG, 2009. p.91–140.